Mol. Cells *27*, 673-680, June 30, 2009
DOI/10.1007/s10059-009-0089-9

Molecules and Cells

Disulfide Bond as a Structural Determinant of Prion Protein Membrane Insertion

Jae Yoon Shin, Jae Il Shin, Jun Seob Kim, Yoo Soo Yang, Yeon-Kyun Shin[1], Kyeong Kyu Kim[2], Sangho Lee[3], and Dae-Hyuk Kweon*

Conversion of the normal soluble form of prion protein, PrP (PrP^C), to proteinase K-resistant form (PrP^{Sc}) is a common molecular etiology of prion diseases. Proteinase K-resistance is attributed to a drastic conformational change from α-helix to β-sheet and subsequent fibril formation. Compelling evidence suggests that membranes play a role in the conformational conversion of PrP. However, biophysical mechanisms underlying the conformational changes of PrP and membrane binding are still elusive. Recently, we demonstrated that the putative transmembrane domain (TMD; residues 111-135) of Syrian hamster PrP penetrates into the membrane upon the reduction of the conserved disulfide bond of PrP. To understand the mechanism underlying the membrane insertion of the TMD, here we explored changes in conformation and membrane binding abilities of PrP using wild type and cysteine-free mutant. We show that the reduction of the disulfide bond of PrP removes motional restriction of the TMD, which might, in turn, expose the TMD into solvent. The released TMD then penetrates into the membrane. We suggest that the disulfide bond regulates the membrane binding mode of PrP by controlling the motional freedom of the TMD.

INTRODUCTION

Prion diseases, which are also termed transmissible spongiform encephalopathies (TSEs), are infectious disorders affecting the brains of humans and animals. In prion diseases, a portion of prion protein (PrP) converts from its normal conformation, PrP^C, to an insoluble and protease-resistant pathogenic conformation, PrP^{Sc} (Prusiner, 1998). Compelling evidence supports the suggestion that PrP^{Sc} might be the transmissible element in prion disease (Castilla et al., 2005; Kocisko et al., 1994; Legname et al., 2004).

Mature mammalian prion proteins are molecules of approximately 209 residues with one conserved disulfide bond between Cys179 and Cys214 (human PrP numbering) (Prusiner, 1998). Structures determined by nuclear magnetic resonance for recombinant PrP^C from human (Zahn et al., 2000), cow (Lopez Garcia et al., 2000), mouse (Riek et al., 1996) and hamster (James et al., 1997) have the same monomeric structure. In contrast, a crystal structure for human prion protein has revealed a three-dimensional domain-swapped dimer (Knaus et al., 2001). All structures contain three α-helices and two strands of β-sheet, with a single disulfide bond bridging helices 2 and 3. While PrP^C is mainly composed of α-helix, conversion to a predominantly β-sheet conformation is the central event of TSEs.

There is evidence that the polypeptide chain of PrP interacts with phospholipid membrane domains. The binding of PrP to a membrane results in structural changes of PrP, with the extent and nature of these structural changes depending on pH, membrane lipid composition and starting construct and conformation of PrP (Critchley et al., 2004; Kazlauskaite et al., 2003; Morillas et al., 1999; Pinheiro, 2006; Sanghera and Pinheiro, 2002; Wang et al., 2006). Furthermore, binding of PrP with a membrane destabilizes the integrity of the lipid bilayer (Kazlauskaite and Pinheiro, 2005; Pinheiro, 2006; Wang et al., 2006). A recent report that utilized a minimal set of components using protein misfolding cyclic amplification identified only PrP molecule, lipid molecules and a synthetic polyanion for scrapie amplification (Deleault et al., 2007). In addition to the membrane localization via the GPI anchor of PrP^C, transmembrane topologies of PrP^C have been described (Hegde et al., 1998; 1999). These transmembrane forms are inserted into the lipid bilayer of the endoplasmic reticulum via the putative transmembrane domain (TMD) of PrP^C, a hydrophobic stretch between residues H^{111} to V^{135}. The first link between this TMD and prion disease became apparent by the observation that a peptide encompassing amino acids 106-126 induces neurotoxic effects in cultured primary brain cells (De Gioia et al., 1994; Forloni et al., 1993).

Recently, we demonstrated that PrP can penetrate into a membrane when the single disulfide bond is reduced (Shin et al., 2008). Insertion of PrP with the membrane upon reduction resulted in the perturbation of the membrane structure, which subsequently lead to leakage of the membrane contents and coprecipitation of the membrane with PrP. Identification of proteinase K (PK)-resistant bands from the membrane-penetrated PrP suggested that the TMD of PrP was inserted to the mem-

Department of Genetic Engineering, Sungkyunkwan University, Suwon 440-746, Korea, [1]Department of Biochemistry and Biophysics, Iowa State University, IA 50011, USA, [2]Department of Molecular Cell Biology, Samsung Biomedical Research Institute, and Sungkyunkwan University School of Medicine, Suwon 440-746, Korea, [3]Department of Biological Science, Sungkyunkwan University, Suwon 440-746, Korea
*Correspondence: dhkweon@skku.edu

Received February 23, 2009; revised April 21, 2009; accepted April 22, 2009; published online June 12, 2009

Keywords: disulfide bond, membrane binding, prion protein, transmembrane domain

brane. These findings lead us to speculate that the TMD, presumably possessing a confined conformation, should gain a degree of motional freedom to interact with the membrane upon reduction of the disulfide bond. In fact, the motion of TMD is likely to be restricted in PrP^{C} in a conformation that obviates interaction with the membrane (James et al., 1997; Shin et al., 2008). In the present study, we compared the structure and membrane binding ability of wild type (WT) Syrian Hamster PrP with a mutant in which two cysteines are replaced with serine residues. The results suggest that the membrane interaction of PrP is enhanced by acquired motional freedom of TMD following the reduction of disulfide bond.

MATERIALS AND METHODS

Materials

1-Palmitoyl-2-oleoyl phosphatidylcholine (POPC) and 1,2-dioleoyl phosphatidylserine (DOPS) were purchased from Avanti Polar Lipids (USA). (1-Oxyl-2,2,5,5-tetramethylpyrrolinyl-3-methyl) methanethiosulfonate spin label (MTSSL) was obtained from Toronto Research Chemicals (Canada). *Pfu* Turbo DNA polymerase was purchased from Stratagene (USA). Bio-beads SM2 was obtained from Bio-Rad (USA). Oligonucleotides for site-directed mutagenesis were obtained from Bioneer (Korea).

Protein expression and purification

The C-terminal fragment spanning residues 90-231 of Syrian Hamster PrP was expressed from pET28a-PrP(90-231) in *Escherichia coli* BL21(DE3). The inclusion body of PrP was refolded as described previously (Shin et al., 2008). Refolded proteins were eluted with 20 mM Tris-HCl pH 7.4 (buffer A) supplemented with 500 mM NaCl and 500 mM imidazole. The solution was centrifuged to remove precipitates. Finally, salts were removed from solution using PD-10 desalting column (GE Healthcare, Buckinghamshire, UK).

Site-specific spin labeling and electron paramagnetic resonance (EPR) data collection

In order to remove or introduce the two cysteine residues, site-directed mutagenesis was performed using *Pfu* polymerase and mutagenic primers. For the nitroxide labeling required for site-directed spin labeling (SDSL) EPR, 1-ocyl-2,2,5,5-tetramethylpyroline-3-methyl methanethiosulfonate (MTSSL) was used. Cys-mutants were incubated overnight with MTSSL at ambient temperature. Free spin labels were removed using a PD10 desalting column (GE Healthcare). Residual free spin labels were washed away using a centrifugal filtration unit (Millipore, USA). EPR spectra were obtained using a Bruker ESP 300 spectrometer (Bruker, Germany) equipped with a low-noise microwave amplifier (Miteq, Hauppauge, USA) and a loop-gap resonator (Medical Advances, USA). The modulation amplitude was set at no greater than one-fourth of the line width. Spectra were collected at room temperature in the first-derivative mode. After baseline correction, the first-derivative EPR spectra were normalized by dividing the spectra with the spin label concentrations. The spin label concentration was obtained from the area of an absorption-mode EPR spectrum, which is double integration value of the first-derivative EPR spectra.

Far-ultraviolet (UV) circular dichroism (CD)

CD spectra of PrP (0.15 mg/ml in 10 mM sodium acetate buffer, pH 7.4) were recorded using a 0.1 cm pathlength cuvette in a CD spectrometer (Jasco, USA) with a bandwidth of 1 nm and data spacing of 0.1 nm. Spectra were measured at 25°C with resolution of 0.5 nm and 16 scans were averaged per spectrum.

Liposomes

Large unilamellar vesicles (LUV) were prepared by hydrating the required amount of dried lipid with the desired buffer (25 mM HEPES, pH 7.0). Buffer was deoxygenated with nitrogen gas and the hydrated lipids were maintained under a nitrogen atmosphere. Phospholipids in chloroform solutions were dried under nitrogen gas and the resulting lipid film was left under vacuum overnight to remove residual chloroform. After lipid hydration, the resulting multilamellar liposome suspension was frozen and thawed 10 times. Finally, the resulting solution was extruded with a 100 nm pore size filter membrane (Avanti Polar Lipids) to generate LUV with a 100 nm diameter.

Generation of polydiacetylene-lipid

Tricosadiynoic acid was purchased from Fluka. Polydiacetylene (PDA) and Phospholipids/PDA LUV consisted of POPC (65% of lipids), DOPS (35% of lipids) and tricosadiynoic acid (lipid to PDA molar ratio of 2:3). The lipid constituents were dried to make a film together in vacuo, followed by addition of deionized water and sonication for 2-3 min at 70°C. The vesicle solution was cooled and kept at 4°C overnight, and then polymerized by cross-linking under UV illumination at 220 nm for 10-20 s. The resulting solutions exhibited an intense blue color.

Fluorescence quenching assay

Fluorescence quenching experiments were performed by adding aliquots of a freshly prepared 2 M acrylamide stock solution to PrP in the absence and presence of membrane. Tryptophan fluorescence spectra were recorded for each quencher concentration using an excitation wavelength at 285 nm (1 nm bandwidth). Protein and lipid concentrations were 1 μM and 2.5 mM, respectively. The degree of quenching was analyzed according to the following Stern-Volmer equation:

$$F_0/F = 1 + K_{SV}[Q] \quad \text{(Eq. 1)}$$

where *F*o and *F* are the fluorescence intensities measured in the absence and presence of acrylamide, respectively, K_{SV} is the Stern-Volmer constant for collisional quenching, and [Q] is the concentration of the quencher. The equation predicts a linear behavior of *Fo*/*F versus* [Q] for a homogeneous solution.

RESULTS

Aggregation-prone property of PrP^{CS} and membrane binding ability

A PrP mutant, in which two cysteines were replaced with serines, was prepared and designated as PrP^{CS}. PrP^{CS} is expected to represent the characteristics of reduced PrP. In recombinant *E. coli* both WT PrP and PrP^{CS} were expressed as inclusion bodies. After purification of unfolded PrPs using Ni-NTA Sepharose, they were subjected to the same solid state refolding processes. While WT PrP could be eluted as a soluble form after refolding, PrP^{CS} could not (Fig. 1A). To understand if this failure in soluble elution was due to the lack of disulfide bond, soluble WT PrP was treated with dithiothreitol (DTT). PrP aggregated very fast depending on the concentration of DTT (Fig. 1B). The precipitates of PrP^{CS} were not PK-resistant indicating that the precipitates were normal amorphous protein aggregates (Fig. 1C). Consistent with previous observations (Maiti and Surewicz, 2001; Mehlhorn et al., 1996), PrP became aggregation-prone when the disulfide bond was reduced.

Tryptophan (Trp) residues provide a convenient spectro-

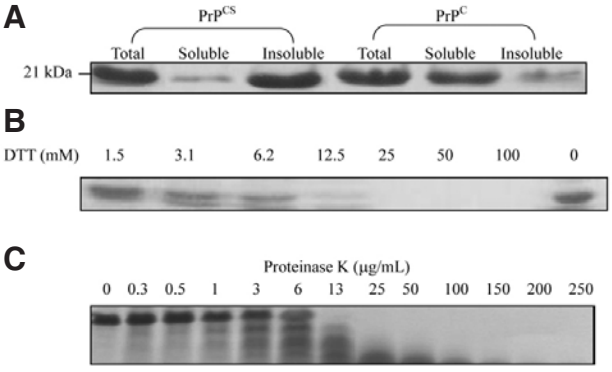

Fig. 1. Aggregation-prone property of PrP^{CS}. (A) PrP^{CS} aggregated rapidly upon elution after the same refolding process as WT PrP which remained soluble after elution. (B) Addition of DTT induced fast aggregation of WT PrP. (C) The precipitates of PrP^{CS} were PK-sensitive. All experiments were carried out in 20 mM Tris-HCl (pH 7.4).

scopic probe that allows the measurement of accessibility to a polar environment at relatively low protein concentration by fluorescence spectroscopy. PrP_{90-231} contains two Trp residues at residues 99 and 146. The putative TMD resides between these two Trp residues. Thus, accessibility to TMD is likely to be well reported by the accessibility to the two Trp residues. Fortunately, we could recover a few μM soluble PrP^{CS}, which was a concentration sufficient to perform fluorescence spectroscopy (Fig. 1A). Fluorescence emission spectra were measured for WT PrP and PrP^{CS} in a wavelength range of 320-400 nm. Interestingly, further exposure of Trp residues to the polar environment was observed for PrP^{CS}, as indicated by the red-shift of λ_{max} (Fig. 2A). Trp exposure is indicative of the exposure of TMD. To confirm the further exposure of Trp residues of PrP^{CS}, fluorescence quenching was measured using acrylamide, which is a polar quencher (Eftink and Ghiron, 1981). PrP^{CS} was more sensitive to acrylamide indicating that the Trp residues of PrP^{CS} were in a more polar environment than those of WT PrP (Fig. 2B).

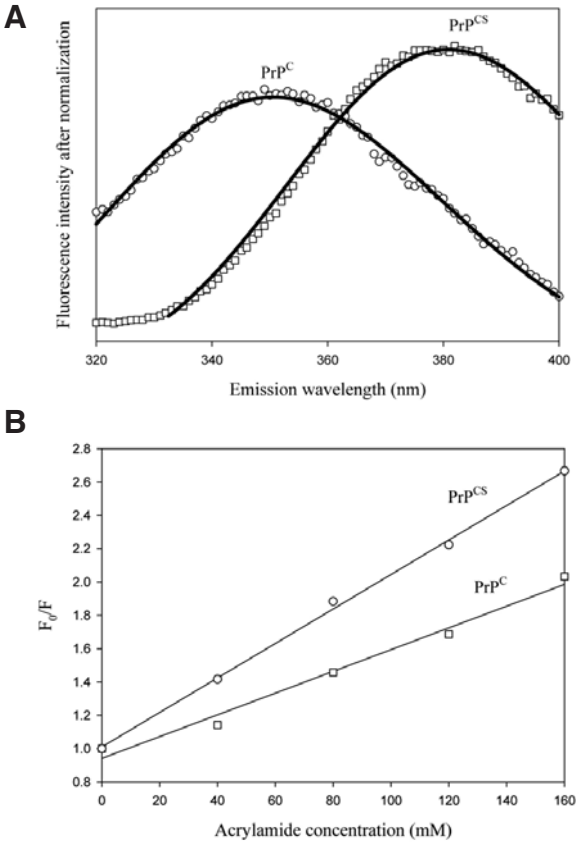

Fig. 2. Accessibility of the putative TMD to polar environment. (A) Red-shift of fluorescence emission spectra indicating that the TMD between the two Trp residues is located in more polar environment when the disulfide bond is missing. (B) Stern-Volmer plot indicating that a water soluble acrylamide is more readily accessible to Trp residues in PrP^{CS} than in PrP^{C}, suggesting that the TMD is exposed when the disulfide bond is lacking.

Membrane insertion of PrP^{CS}

In our previous report, membrane interaction of PrP strongly depended on the redox state of the disulfide bond (Shin et al., 2008). It was of interest to determine whether PrP^{CS} could still retain its membrane binding ability. As expected, we observed potent membrane binding when the disulfide bond was missing. To characterize the interaction between PrPs and membrane lipids, we used the technique of fluorescence quenching with acrylamide. Figure 3A shows representative Stern-Volmer plots for acrylamide quenching of Trp fluorescence of WT PrP and PrP^{CS} in the presence or absence of membrane. WT PrP was sensitive to the fluorescence polar quencher acrylamide. Acrylamide quenching of WT PrP was not protected in the presence of membrane. These result are consistent with the suggestion that WT PrP does not bind to membrane at neutral pH and agrees with previous observations (Morillas et al., 1999), in which WT PrP_{90-231} showed appreciable affinity for lipids only at acidic pH. However, PrP^{CS} showed dramatic membrane binding ability even at neutral pH. The acrylamide quencher was almost completely blocked from access to Trps of PrP^{CS} clearly indicating that TMD inserted into the membrane.

In our previous report, WT PrP perturbed the membrane structure, inducing leakage of contents when the disulfide bond was reduced (Shin et al., 2008). Presently, membrane disruption by PrP was shown using phospholipid/PDA membranes. Phospholipid/PDA membranes have been shown to undergo distinct blue-red colorimetric changes owing to conformational transitions in the conjugated (ene-yne) polymer backbone when structural perturbations are externally introduced. Presently, phospholipid/PDA membranes underwent a colorimetric change from blue to red upon addition of PrP^{CS} (Fig. 3B, circles). In contrast, WT PrP did not induce a colorimetric change (squares). Consequently, we could observe strong absorption at approximately 550 nm only after addition of PrP^{CS}.

EPR spectroscopy

The disulfide-lacking mutant, PrP^{CS}, still retained membrane-binding ability that was related to aggregation-prone propensity in solution. WT PrP was soluble at a high concentration but did not interact with membrane efficiently. We assumed that the putative TMD could be relieved from motional restriction by reduction of the disulfide bond. In turn, the exposed hydrophobic TMD would drive aggregation of PrP molecules in solution. But, in the presence of membrane, the exposed TMD would have another option, namely membrane insertion. However, it was still questionable whether the reduction of disulfide bond could induce a structural change that was sufficient to allow the movement of the TMD.

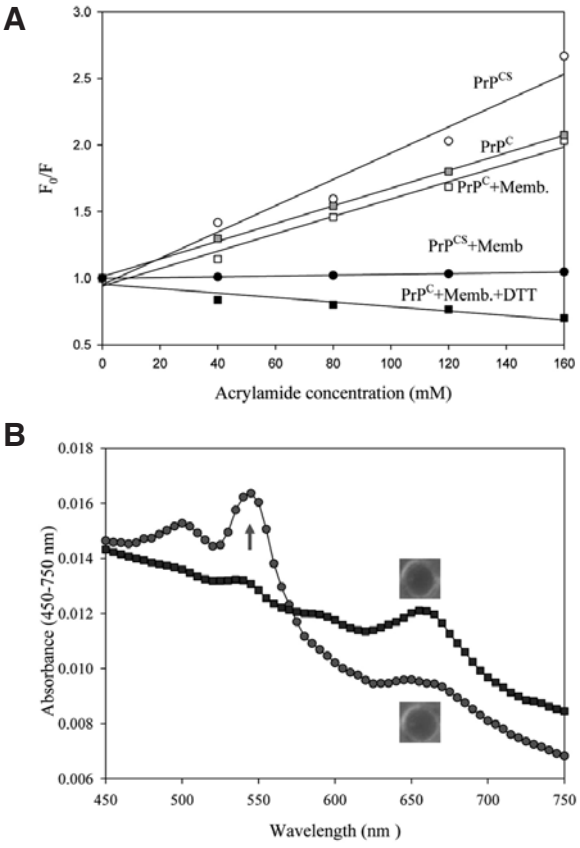

Fig. 3. Membrane binding ability of PrP^{CS}. (A) Stern-Volmer plots indicating that the soluble acrylamide quencher is not accessible to Trp residues when the disulfide bond is lacking. Exposed TMD (open circle) was shielded from acrylamide in the presence of membrane indicating membrane insertion. (B) Phospholipids/PDA membrane changed color upon the addition of PrP^{CS}, while the addition of WT PrP did not induce colorimetric change. As a result, PrP^{CS}-induced structural change of phospholipid/PDA membrane demonstrated a strong absorbance at approximately 550 nm.

SDSL EPR spectroscopy has been used to determine structures of various membrane proteins. EPR spectrum is sensitive to the motional rate of spin label attached to the protein and its lineshape analysis provides information about local structure (Fanucci and Cafiso, 2006; Hubbell et al., 1996; 2000; McHaourab et al., 1999). Thus, SDSL EPR is expected to pinpoint whether the release of TMD is accompanied by the increase in the motional rate of other region of PrP.

For SDSL EPR spectroscopy, 2 sets of seven spin labeling mutants were prepared (Fig. 4A). Spin labeling mutants comprised one mutant (148C) for helix 1, six mutants for long helix 2 (177C, 186C and 190C) and helix 3 (205C, 211C and 22C). Two identical mutation sets were prepared using WT PrP and PrP^{CS}. Spin label mutants grafted on WT PrP probes PrP conformation with disulfide bond, while spin label mutants of PrP^{CS} are representative of reduced state of PrP. First, EPR spectra for seven spin labeling mutants grafted on WT PrP were measured at room temperature. As nitroxide was labeled to α-helices, we could observe relatively broad lineshapes from all spin label positions (Fig. 4B), which were the typical spectra expected from secondary structures (Hubbell et al., 1996; 2000). Unfortunately, EPR analysis of PrP^{CS} was more complicated because PrP^{CS} could not be recovered in a soluble form at high concentration (Fig. 1). For a typical SDSL EPR experiment, 50-100 μM protein is applied. To dissolve PrP^{CS} in solution at high concentration, various additives were supplemented into buffer A. Among 0.2% Triton X-100, 0.2% Tween 20, 0.2% *n*-octyl-glucoside, 3 M urea, 0-3 M NaCl, 100% dimethylsulfoxide, 50 mM cholic acid, 1.5 M guanidinium hydrochloride (GdmHCl) and 0.3% sodium dodecyl sulfate (SDS) and 50% tetrafluoroethylene (TFE), only GdmHCl and SDS were effective for soluble elution of PrP^{CS} (data not shown). In 50% TFE, PrP^{CS} was soluble only temporarily (significant aggregation within 10 min after elution). Because it was reported that 1.5M GdmHCl does not unfold PrP_{90-231} at neutral pH (Swietnicki et al., 1997), we chose GdmHCl for soluble elution of PrP^{CS}.

Normalized EPR spectra for WT PrP and PrP^{CS} in 1.5 M GdmHCl (pH 7.0) were overlapped for comparison of their motional rate (Fig. 4C, left row). One might expect lower peak heights from broader spectra after normalization. On the contrary, faster motion and sharper lineshape will show taller peak heights in the normalized spectra. Overlapped spectra clearly indicated that spin labels on PrP^{CS} moved faster than those on WT PrP (Fig. 3C, left row). It can be argued that GdmHCl might also disturb WT PrP structure, although 1.5 M GdmHCl was indispensable for soluble maintenance of PrP^{CS}. EPR spectra of WT PrP in buffer A were also superimposed with those of WT PrP in 1.5 M GdmHCl (Fig. 3C, right row). Addition of GdmHCl produced comparably similar lineshapes, indicating that the reduction of disulfide bond contributed to the increase in the motional rate much more than GdmHCl. This became more obvious with the comparison of the ratio of first peak heights (Fig. 4D). The height of the first peak (H1) in a normalized spectrum is a clear indication of the sharpness of a lineshape especially when central linewidth (H0) is not clear (Kweon et al., 2006). As expected from Fig. 4B, EPR spectra for WT PrP were mostly composed two components; one from helix and the other from fast moving structure, perhaps sharp components derived from incomplete formation of the disulfide bond. These composite spectra often blur the calculation of H0. Thus, H1 gives rise to more precise comparison than H0. In Fig. 4D, the ratios of H1 was 2.5-4 when the disulfide bond was reduced, while those were 0.8-2.2 in the presence of GdmHCl (ratio of 1 indicates no change). Helix 2 of PrP showed the most dramatic changes in motional rate upon the reduction of disulfide bond but helix 3 did not show significant changes in the motional rate.

Finally, we measured conformational change of PrP^{CS} occurring upon membrane insertion using SDSL EPR and CD spectroscopy (Fig. 5). Spin label mutants of PrP^{CS} dissolved in 0.3% SDS were mixed with membrane. Then, membrane insertion was induced by rapid dilution by adding three volumes of buffer A followed by removal of detergent using Bio-Beads SM2. After removing large aggregates by centrifugation, supernatants were subjected to EPR analysis. In the membrane, all spin label mutants showed significantly broad EPR spectra (Fig. 5A, left row). The extent of spectral broadening depended on the spin labeling position. For example, 205*/PrP^{CS} showed strong immobile component (solid arrow), an indication of tertiary contact. Spin label mutants177*/PrP^{CS}, 203*/PrP^{CS} and 211*/PrP^{CS} (triangle) showed a signal of dipolar interaction, and others showed typical spectra of exposed secondary structure. The signal of dipolar interaction, tertiary interaction and exposed secondary structure were indicative of a new conformation in the membrane. In marked contrast, all spin labeling mutants of PrP^{CS} dissolved in SDS showed almost identical EPR spectral lineshapes (Fig. 5A, right row). The aggregate of 222*/PrP^{CS}

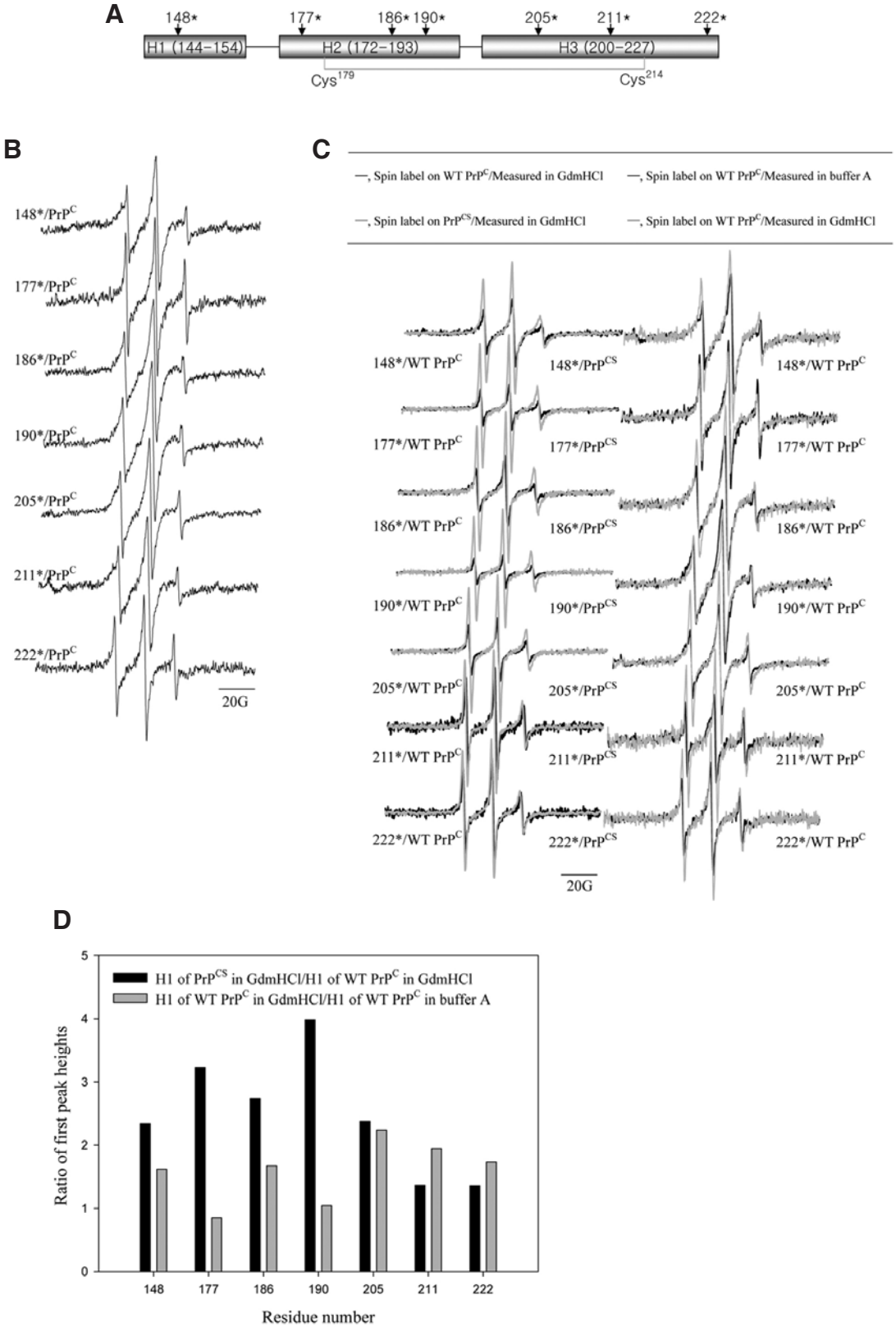

Fig. 4. EPR spectroscopy of WT PrP and PrP^{CS}. (A) Schematic diagram of spin-labeling positions. Each bar represents helices. There is an intramolecular disulfide bond between C^{179} and C^{214}. Asterisks denote spin-labeled residues. (B) Room temperature derivative EPR spectra of seven spin label mutants of WT PrP. (C) Superimposed EPR spectra. Left row, WT PrP^{C} in GdmHCl vs. PrP^{CS} in GdmHCl; right row, WT PrP^{C} in buffer A vs. WT PrP^{C} in GdmHCl. (D) Comparison of ratio of first peak heights (H1).

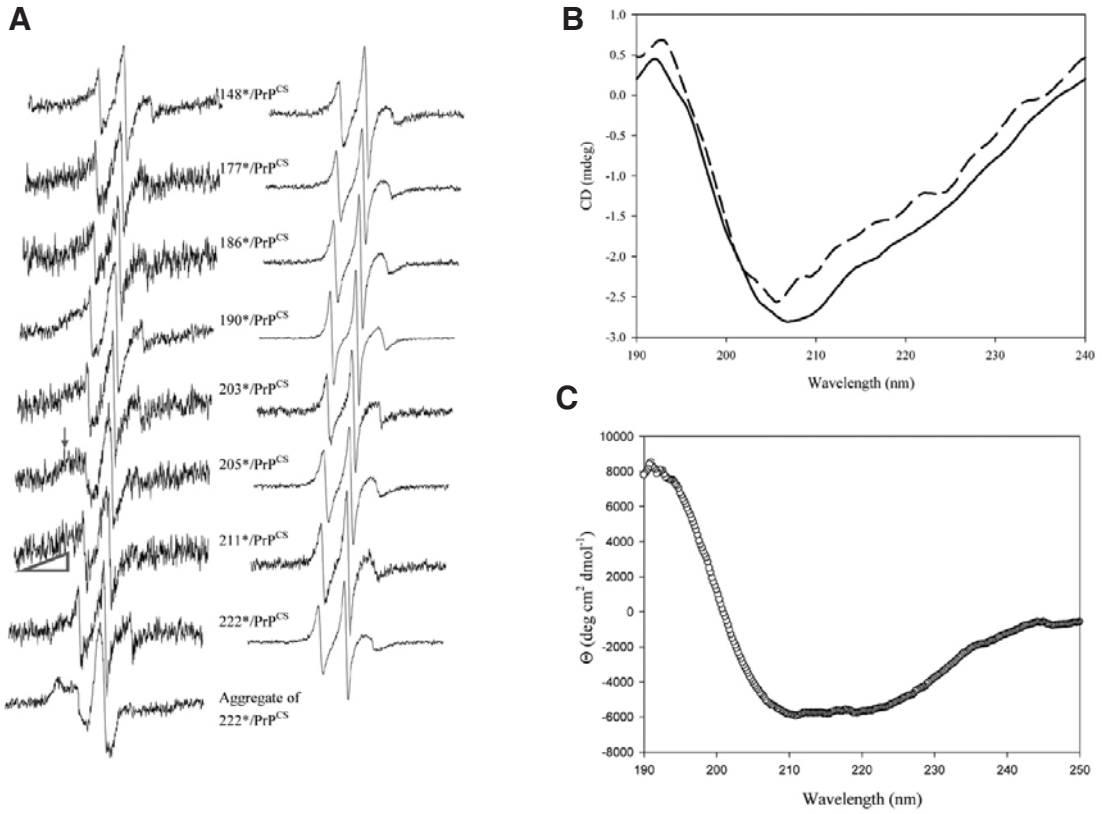

Fig. 5. Conformational change of PrP^{CS} in the membrane. (A) Derivative EPR spectra of spin label mutants of PrP^{CS} in the membrane (left row) or in SDS (right row). Arrow indicates the appearance of immobile component suggesting tertiary contact. Triangle indicates dipolar interaction that suggests oligomerization of those points. (B) CD spectra of PrP^{CS} in the presence of 0.3% SDS (broken line) and 5 mM membrane (solid line). (C) CD spectra of WT PrP^{C}. The initial concentration of the samples was 0.15 mg/mL in 10 mM sodium acetate, pH 7.4. Figure B was not converted to molar ellipticity because the protein concentration in SDS or in the membrane could not be precisely measured.

prepared by simply removing SDS without membrane and collecting by centrifugation contained a very strong immobile component in the EPR spectrum and an apparent hyperfine splitting (the lowest spectrum of Fig. 5A). Totally different spectra between the membrane-inserted PrP and the simple aggregate ruled out the possibility that the spectra for 148*-222* were the aggregation products of PrP^{CS}s.

CD spectra of PrP^{CS} in the membrane context clearly showed reduced helical contents without any indication of increased β-sheet contents when compared to those of PrP^{C} (Figs. 5B and 5C). Two minima at 208 nm and 222 nm in the CD spectra of WT PrP^{C} were an indication of its helical contents (Fig. 5C). The minimum at 222 nm diminished in the CD spectra of PrP^{CS} in the presence of 0.5% SDS or 5 mM membrane while the minimum at 208 nm weakened to some extent (Fig. 5B). The CD data were consistent with the suggestion that in the membrane PrP^{CS} loosens a significant portion of its helices when the disulfide bond of PrP is reduced. Taken together with the EPR data, it is plausible to suggest that PrP reorients to form a new conformation in the membrane with a significant loss of helical property. It is not clear at this time whether this conformation will change eventually into a β-sheet-rich conformation after prolonged incubation as SDS does (Stohr et al., 2008).

DISCUSSION

The interaction between cytoplasmic PrP and the hydrophobic lipid core of membrane correlates with neurotoxicity (Wang et al., 2006). Previous studies revealed PrP interaction with lipids (Baron and Caughey, 2003; Critchley et al., 2004; Kazlauskaite et al., 2003; Morillas et al., 1999; Sanghera and Pinheiro, 2002) and that recombinant PrP can bind and disrupt liposomes composed of negatively charged phospholipids (Kazlauskaite et al., 2003). Recently, we demonstrated that the membrane interaction mode is regulated by the disulfide bond of PrP (Shin et al., 2008). In the present study, we show the structural feature of this membrane binding mode that relies on disulfide bond reduction. Fluorescence spectroscopy showed that the putative TMD is exposed upon reduction of disulfide bond (Fig. 2). The released TMD has two options to shield its hydrophobic region; aggregation with other PrP molecules in the absence of membrane (Fig. 1) or insertion into the membrane in the presence of membrane (Figs. 3 and 6). EPR spectroscopy showed that the helix 2 gained the largest motional freedom upon disulfide bond reduction (Fig. 4D). This increased motional freedom allows the exposure of the TMD, which, in turn, enables membrane interaction. After insertion into the membrane, PrP forms a new conformation and is accompanied by the loss of α-helical contents, but not by an increase of β-sheet (Fig. 5). Our observation is consistent with the strong membrane binding at neural pH observed by other group that accompanies marked unfolding, extensive aggregation and oligomerization (Re et al., 2008). Thus, the disulfide bond of PrP seems to be the structural determinant of membrane binding of PrP. Our present study also

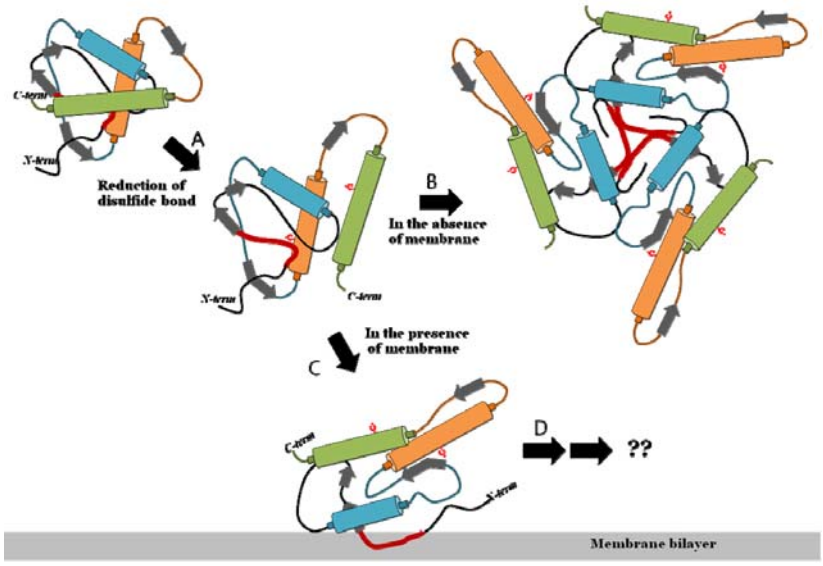

Fig. 6. Membrane insertion of PrP regulated by disulfide bond. (A) The putative TMD (thick red line) is shielded from solution in the oxidized PrP. Reduction of disulfide bond induces global structural change of PrP that accompanies the increased motional freedom of the TMD. Especially, helix 2 becomes the fastest moving of the three helices. (B) In the absence of membrane, PrP becomes aggregation-prone by the released TMD interaction. (C) In the presence of membrane, the released TMD penetrates into the membrane. (D) Perhaps, the membrane-inserted PrP changes into β-sheet-rich conformation after long period of incubation as SDS does (Stohr et al., 2008), or forms a channel (Lin et al., 1997).

suggests that the pH-dependent membrane binding ability of previous reports might be the indirect consequence of pH-dependent equilibrium change of the disulfide bond.

The role of disulfide bond of PrP is still controversial. In PrP^C, a disulfide bond stabilizes the overall fold of the protein by connecting the two long helices (Zahn et al., 2000). Some experiments have suggested that the disulfide bond of PrP^C is reduced during the conversion (Horiuchi and Caughey, 1999; Jackson, 1999; Welker et al., 2001). In contrast, it was also proposed that the presence of this sole intramolecular disulfide bond in PrP^C is required for conversion to PrP^{Sc} (Maiti and Surewicz, 2001; Muramoto et al., 1996; Welker et al., 2002). The disulfide bond might not be broken even temporarily (Welker et al., 2002). On the other hand, the cysteines of PrP^{Sc} are assumed to be involved in a disulfide bond because denaturant-solubilized PrP^{Sc} reacts with thiol-specific reagents only after treatment with reducing agents (Turk et al., 1988), suggesting that the possible reduction of this disulfide bond may be a temporary event. It was also reported that upon reduction of a single disulfide bridge the recombinant PrP can reversibly switch between α-helical conformation and a monomeric form rich in β-sheet structure at low pH (Jackson, 1999). It was postulated that the latter form represented a key monomeric precursor of PrP^{Sc}. Meanwhile, another experiment failed to confirm the same result but argued against the notion that reduced PrP could exist in a stable monomer that is rich in β-sheet structure at low pH (Maiti and Surewicz, 2001). Whether the disulfide bonds in PrP^{Sc} are intermolecular between monomers or intramolecular within a monomer is a critical issue that has important consequences for understanding the molecular mechanism of the conformational transition. Here, we report that membrane binding, believed to be a crucial factor in the conformational transition, is controlled by a single disulfide bond. Determination of membrane structure of the TMD deserves further investigation.

Since PrP^C is predominantly sequestered into lipid raft domains which are rich in cholesterol and sphingomyelin, raft is believed to play a role in the prion conversion. In support of this notion, both PrP^C and PrP^{Sc} co-localize in rafts, cholesterol depletion decreases formation of PrP^{Sc} in prion-infected cell lines, depletion of sphingolipids destabilizes rafts and increases the formation of PrP^{Sc}, and transmembrane forms of PrP^C not localized in rafts does not serve as substrate for the formation of PrP^{Sc}. Based on these some ambivalent effects of raft on PrP conversion it might be assumed that the initial conversion process occur outside rafts and then re-enter rafts to form a mature PrP^{Sc}. In line with this assumption, the transmembrane form of PrP is not necessarily present in rafts. A recent report also showed that the TMD interaction did not show any preference to the membrane structure but depended on pH (Re et al., 2008). Thus, specific membrane structure such as rafts does not seem to affect the selectivity of TMD-membrane interaction.

The role of PrP-membrane interaction is still controversial. Membrane might merely play a role in the conversion of PrP^C to PrP^{Sc} (Critchley et al., 2004; Kazlauskaite et al., 2003; Morillas et al., 1999; Pinheiro, 2006; Sanghera and Pinheiro, 2002) or directly affect cell physiology leading to cell death (De Gioia et al., 1994; Forloni et al., 1993; Lin et al., 1997; Wang et al., 2006). Thermodynamics and kinetics study seem to be needed to elucidate the role of membrane on PrP conversion because we do not know yet whether membrane would affect conversion rate constant or equilibrium constant. Furthermore, the structure of the putative TMD in membrane needs to be determined, which will give us insight into the function of PrP-membrane interaction and pathogenesis mechanism.

ACKNOWLEDGMENT

This work was supported by Korea Research Foundation Grant (KRF-2004-C00316).

REFERENCES

Baron, G.S., and Caughey, B. (2003). Effect of glycosylphosphatidylinositol anchor-dependent and -independent prion protein association with model raft membranes on conversion to the protease-resistant isoform. J. Biol. Chem. *278*, 14883-14892.

Castilla, J., Saa, P., Hetz, C., and Soto, C. (2005). *In vitro* generation of infectious scrapie prions. Cell *121*, 195-206.

Critchley, P., Kazlauskaite, J., Eason, R., and Pinheiro, T.J. (2004). Binding of prion proteins to lipid membranes. Biochem. Biophys. Res. Commun. *313*, 559-567.

De Gioia, L., Selvaggini, C., Ghibaudi, E., Diomede, L., Bugiani, O., Forloni, G., Tagliavini, F., and Salmona, M. (1994). Conformational polymorphism of the amyloidogenic and neurotoxic peptide homologous to residues 106-126 of the prion protein. J. Biol. Chem. *269*, 7859-7862.

Deleault, N.R., Harris, B.T., Rees, J.R., and Supattapone, S. (2007). From the cover: formation of native prions from minimal compo-

nents *in vitro*. Proc. Natl. Acad. Sci. USA *104*, 9741-9746.
Eftink, M.R., and Ghiron, C.A. (1981). Fluorescence quenching studies with proteins. Anal. Biochem. *114*, 199-227.
Fanucci, G.E., and Cafiso, D.S. (2006). Recent advances and applications of site-directed spin labeling. Curr. Opin. Struct. Biol. *16*, 644-653.
Forloni, G., Angeretti, N., Chiesa, R., Monzani, E., Salmona, M., Bugiani, O., and Tagliavini, F. (1993) Neurotoxicity of a prion protein fragment. Nature *362*, 543-546.
Hegde, R.S., Mastrianni, J.A., Scott, M.R., DeFea, K.A., Tremblay, P., Torchia, M., DeArmond, S.J., Prusiner, S.B., and Lingappa, V.R. (1998). A transmembrane form of the prion protein in neurodegenerative disease. Science *279*, 827-834.
Hegde, R.S., Tremblay, P., Groth, D., DeArmond, S.J., Prusiner, S.B., and Lingappa, V.R. (1999). Transmissible and geneti prion diseases share a common pathway of neurodegeneration. Nature *402*, 822.
Horiuchi, M., and Caughey, B. (1999). Prion protein interconversions and the transmissible spongiform encephalopathies. Structure *7*, R231-240.
Hubbell, W.L., McHaourab, H.S., Altenbach, C., and Lietzow, M.A. (1996). Watching proteins move using site-directed spin labeling. Structure *4*, 779-783.
Hubbell, W.L., Cafiso, D.S., and Altenbach, C. (2000). Identifying conformational changes with site-directed spin labeling. Nat. Struct. Biol. *7*, 735-739.
Jackson, G.S. (1999). Reversible conversion of monomeric human prion protein between native and fibrilogenic conformations. Science *283*, 1935.
James, T.L., Liu, H., Ulyanov, N.B., Farr-Jones, S., Zhang, H., Donne, D.G., Kaneko, K., Groth, D., Mehlhorn, I., Prusiner, S.B., et al. (1997). Solution structure of a 142-residue recombinant prion protein corresponding to the infectious fragment of the scrapie isoform. Proc. Natl. Acad. Sci. USA *94*, 10086-10091.
Kazlauskaite, J., and Pinheiro, T.J. (2005). Aggregation and fibrillization of prions in lipid membranes. Biochem. Soc. Symp. *72*, 211-222.
Kazlauskaite, J., Sanghera, N., Sylvester, I., Venien-Bryan, C., and Pinheiro, T.J. (2003). Structural changes of the prion protein in lipid membranes leading to aggregation and fibrillization. Biochemistry *42*, 3295-3304.
Knaus, K.J., Morillas, M., Swietnicki, W., Malone, M., Surewicz, W.K., and Yee, V.C. (2001). Crystal structure of the human prion protein reveals a mechanism for oligomerization. Nat. Struct. Biol. *8*, 770-774.
Kocisko, D.A., Come, J.H., Priola, S.A., Chesebro, B., Raymond, G.J., Lansbury, P.T., and Caughey, B. (1994). Cell-free formation of protease-resistant prion protein. Nature *370*, 471-474.
Kweon, D.H., Shin, Y.K., Shin, J.Y., Lee, J.H., Lee, J.B., Seo, J.H., and Kim, Y.S. (2006). Membrane topology of helix 0 of the Epsin N-terminal homology domain. Mol. Cells *21*, 428-435.
Legname, G., Baskakov, I.V., Nguyen, H.O., Riesner, D., Cohen, F.E., DeArmond, S.J., and Prusiner, S.B. (2004). Synthetic mammalian prions. Science *305*, 673-676.
Lin, M.C., Mirzabekov, T., and Kagan, B.L. (1997). Channel formation by a neurotoxic prion protein fragment. J. Biol. Chem. *272*, 44-47.
Lopez Garcia, F., Zahn, R., Riek, R., and Wuthrich, K. (2000). NMR structure of the bovine prion protein. Proc. Natl. Acad. Sci. USA *97*, 8334-8339.
Maiti, N.R., and Surewicz, W.K. (2001). The role of disulfide bridge in the folding and stability of the recombinant human prion protein. J. Biol. Chem. *276*, 2427-2431.
McHaourab, H.S., Kalai, T., Hideg, K., and Hubbell, W.L. (1999). Motion of spin-labeled side chains in T4 lysozyme: effect of side chain structure. Biochemistry *38*, 2947-2955.
Mehlhorn, I., Groth, D., Stockel, J., Moffat, B., Reilly, D., Yansura, D., Willett, W.S., Baldwin, M., Fletterick, R., Cohen, F.E., et al. (1996). High-level expression and characterization of a purified 142-residue polypeptide of the prion protein. Biochemistry *35*, 5528-5537.
Morillas, M., Swietnicki, W., Gambetti, P., and Surewicz, W.K. (1999). Membrane environment alters the conformational structure of the recombinant human prion protein. J. Biol. Chem. *274*, 36859-36865.
Muramoto, T., Scott, M., Cohen, F.E., and Prusiner, S.B. (1996). Recombinant scrapie-like prion protein of 106 amino acids is soluble. Proc. Natl. Acad. Sci. USA *93*, 15457-15462.
Pinheiro, T.J. (2006). The role of rafts in the fibrillization and aggregation of prions. Chem. Phys. Lipids *141*, 66-71.
Prusiner, S.B. (1998). Prions. Proc. Natl. Acad. Sci. USA *95*, 13363-13383.
Re, F., Sesana, S., Barbiroli, A., Bonomi, F., Cazzaniga, E., Lonati, E., Bulbarelli, A., and Masserini, M. (2008). Prion protein structure is affected by pH-dependent interaction with membranes: a study in a model system. FEBS Lett. *582*, 215-220.
Riek, R., Hornemann, S., Wider, G., Billeter, M., Glockshuber, R., and Wuthrich, K. (1996). NMR structure of the mouse prion protein domain PrP(121-321). Nature *382*, 180-182.
Sanghera, N., and Pinheiro, T.J. (2002). Binding of prion protein to lipid membranes and implications for prion conversion. J. Mol. Biol. *315*, 1241-1256.
Shin, J.I., Shin, J.Y., Kim, J.S., Yang, Y.S., Shin, Y.K., and Kweon, D.H. (2008). Deep membrane insertion of prion protein upon reduction of disulfide bond. Biochem. Biophys. Res. Commun. *377*, 995-1000.
Stohr, J., Weinmann, N., Wille, H., Kaimann, T., Nagel-Steger, L., Birkmann, E., Panza, G., Prusiner, S.B., Eigen, M., and Riesner, D. (2008). Mechanisms of prion protein assembly into amyloid. Proc. Natl. Acad. Sci. USA *105*, 2409-2414.
Swietnicki, W., Petersen, R., Gambetti, P., and Surewicz, W.K. (1997). pH-dependent stability and conformation of the recombinant human prion protein PrP(90-231). J. Biol. Chem. *272*, 27517-27520.
Turk, E., Teplow, D.B., Hood, L.E., and Prusiner, S.B. (1988). Purification and properties of the cellular and scrapie hamster prion proteins. Eur. J. Biochem. *176*, 21-30.
Wang, X., Wang, F., Arterburn, L., Wollmann, R., and Ma, J. (2006). The interaction between cytoplasmic prion protein and the hydrophobic lipid core of membrane correlates with neurotoxicity. J. Biol. Chem. *281*, 13559-13565.
Welker, E., Wedemeyer, W.J., Narayan, M., and Scheraga, H.A. (2001). Coupling of conformational folding and disulfide-bond reactions in oxidative folding of proteins. Biochemistry *40*, 9059-9064.
Welker, E., Raymond, L.D., Scheraga, H.A., and Caughey, B. (2002). Intramolecular versus intermolecular disulfide bonds in prion proteins. J. Biol. Chem. *277*, 33477-33481.
Zahn, R., Liu, A., Luhrs, T., Riek, R., von Schroetter, C., Lopez Garcia, F., Billeter, M., Calzolai, L., Wider, G., and Wuthrich, K. (2000). NMR solution structure of the human prion protein. Proc. Natl. Acad. Sci. USA *97*, 145-150.